



## **Bone morphogenetic protein 10 is increased in pre-capillary pulmonary hypertension patients**

Llucià-Vallduperas, A.; Wezenbeek, J. van; Groeneveldt, J.A.; Smal, R.; Sánchez-Duffhues, G.; Becher, C.; ... ; Man, F.S. de

### **Citation**

Llucià-Vallduperas, A., Wezenbeek, J. van, Groeneveldt, J. A., Smal, R., Sánchez-Duffhues, G., Becher, C., ... Man, F. S. de. (2025). Bone morphogenetic protein 10 is increased in pre-capillary pulmonary hypertension patients. *Cardiovascular Research*, 121(8), 1254-1268.  
doi:10.1093/cvr/cvaf028

Version: Publisher's Version

License: [Creative Commons CC BY-NC 4.0 license](https://creativecommons.org/licenses/by-nc/4.0/)

Downloaded from: <https://hdl.handle.net/1887/4290268>

**Note:** To cite this publication please use the final published version (if applicable).

# Bone morphogenetic protein 10 is increased in pre-capillary pulmonary hypertension patients

**Aida Llucià-Valdeperas**  <sup>1,2†</sup>, **Jessie van Wezenbeek** <sup>1,2†</sup>, **Joanne A. Groeneveldt** <sup>1,2</sup>, **Rowan Smal** <sup>1,2</sup>, **Gonzalo Sánchez-Duffhues** <sup>3,4</sup>, **Clarissa Becher** <sup>3</sup>, **Azar Kianzad** <sup>1,2</sup>, **Samara M.A. Jansen** <sup>1,2</sup>, **Jeroen N. Wessels** <sup>1,2</sup>, **M. Louis Handoko**  <sup>5</sup>, **Lilian J. Meijboom** <sup>6</sup>, **J. Tim Marcus** <sup>6</sup>, **Petr Symersky** <sup>7</sup>, **Hans W.M. Niessen** <sup>8</sup>, **Anton Vonk-Noordegraaf** <sup>1,2</sup>, **Harm Jan Bogaard** <sup>1,2</sup>, **Marie José Goumans** <sup>3\*‡</sup>, and **Frances S. de Man** <sup>1,2\*‡</sup>

<sup>1</sup>Department of Pulmonary Medicine, Amsterdam UMC location Vrije Universiteit Amsterdam, PHEniX Laboratory, De Boelelaan 1117, 1081HV Amsterdam, The Netherlands; <sup>2</sup>Amsterdam Cardiovascular Sciences, Pulmonary Hypertension and Thrombosis, De Boelelaan 1117, 1081HV Amsterdam, The Netherlands; <sup>3</sup>Department of Cell and Chemical Biology, Leiden UMC, Einthovenweg 20, 2333 ZC Leiden, The Netherlands; <sup>4</sup>Nanomaterials and Nanotechnology Research Center (CINN-CSIC), Health Research Institute of Asturias (ISPA), Av. del Hospital Universitario s/n, 33011 Oviedo, Asturias, Spain; <sup>5</sup>Department of Cardiology, Amsterdam UMC location Vrije Universiteit Amsterdam, De Boelelaan 1117, 1081HV Amsterdam, The Netherlands; <sup>6</sup>Department of Radiology and Nuclear Medicine, Amsterdam UMC location Vrije Universiteit Amsterdam, De Boelelaan 1117, 1081HV Amsterdam, The Netherlands; <sup>7</sup>Department of Cardiothoracic Surgery, Amsterdam UMC location Vrije Universiteit Amsterdam, De Boelelaan 1117, 1081HV Amsterdam, The Netherlands; and <sup>8</sup>Department of Pathology, Amsterdam UMC location Vrije Universiteit Amsterdam, De Boelelaan 1117, 1081HV Amsterdam, The Netherlands

Received 19 February 2024; revised 30 July 2024; accepted 5 December 2024; online publish-ahead-of-print 24 February 2025

**Time for primary review: 35 days**

## Aims

Pre-capillary pulmonary hypertension (precPH) results in increased right atrial (RA) stretch and pressure. The right atrium is the major source of bone morphogenetic protein 10 (BMP10) in adults, primarily produced by RA cardiomyocytes. The aim of this study was to investigate BMP10 expression in the right heart and systemic circulation and to identify potential triggers for increased BMP10 secretion associated with precPH.

## Methods and results

We examined BMP10 mRNA and protein expressions in RA tissue. Circulating BMP10 plasma levels were determined using enzyme-linked immunosorbent assay. BMP10 transcriptional activity was studied using a BMP-responsive element luciferase assay. Correlation analyses were performed between circulating BMP10 and RA dilatation as well as right ventricular (RV) function. Finally, we determined the impact of pressure unloading on BMP10 activity in chronic thromboembolic pulmonary hypertension (CTEPH) patients before and after pulmonary endarterectomy (PEA). BMP10 mRNA's protein and activity were significantly increased in the precPH right atrium. While circulating BMP10 protein levels were elevated, no significant changes were observed in BMP10 transcriptional activity between precPH and controls. Interestingly, RA dilatation, increased RA pressure, high N-terminal pro b-type natriuretic peptide levels, and reduced RV ejection fraction were associated with high BMP10 activity. Finally, pressure unloading after PEA in a cohort of CTEPH patients resulted in reduced BMP10 activity.

## Conclusion

RA BMP10 expression and plasma levels are increased in precPH, likely triggered by excessive RA dilatation and pressure overload. Future studies are needed to determine whether increased BMP10 release is an adaptive mechanism or a potential therapeutic target.

\* Corresponding author. Tel: +31 20 444 1883, E-mail: [fs.deman@amsterdamumc.nl](mailto:fs.deman@amsterdamumc.nl) (F.S.d.M.); Tel: +31 71 526 9277, E-mail: [m.j.t.h.goumans@lumc.nl](mailto:m.j.t.h.goumans@lumc.nl) (M.J.G.)

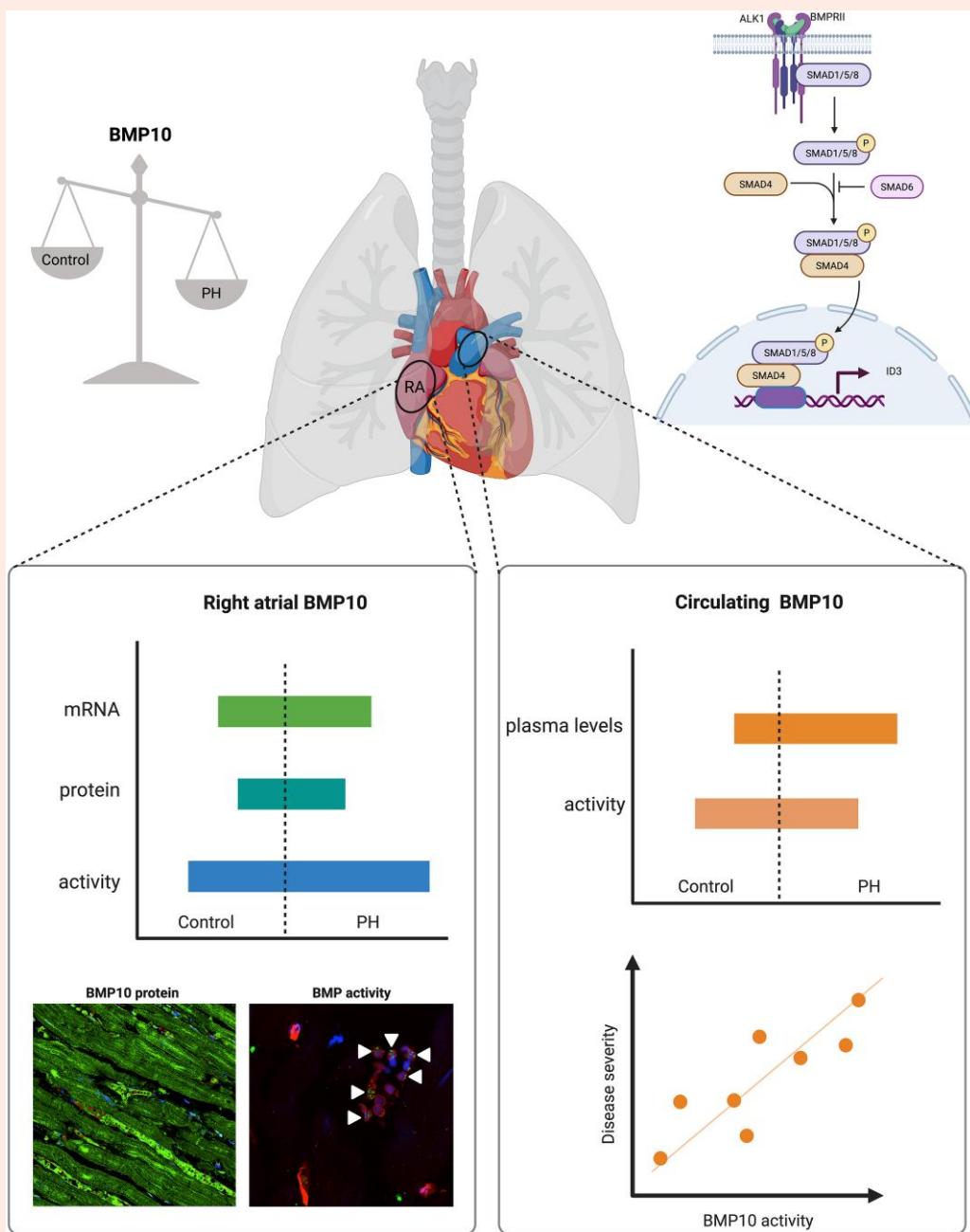
† The first two authors contributed equally to this work.

‡ These authors shared last authorship.

© The Author(s) 2025. Published by Oxford University Press on behalf of the European Society of Cardiology.

This is an Open Access article distributed under the terms of the Creative Commons Attribution-NonCommercial License (<https://creativecommons.org/licenses/by-nc/4.0/>), which permits non-commercial re-use, distribution, and reproduction in any medium, provided the original work is properly cited. For commercial re-use, please contact [reprints@oup.com](mailto:reprints@oup.com) for reprints and translation rights for reprints. All other permissions can be obtained through our RightsLink service via the Permissions link on the article page on our site—for further information please contact [journals.permissions@oup.com](mailto:journals.permissions@oup.com).

## Graphical Abstract



Increased BMP10 in precPH patients compared with controls. Higher BMP10 expression and activity in the right atrium and greater BMP10 expression, but preserved activity, in the circulation. Increased BMP10 activity associates with disease severity. Created with BioRender.com.

### Keywords

BMP • TGF-beta • Pulmonary hypertension • Right atrium • BMP10

## 1. Introduction

Pre-capillary pulmonary hypertension (precPH) is a rare condition characterized by remodelling of pulmonary arterioles leading to progressive overload for the right heart.<sup>1,2</sup> First, the right heart adapts, but eventually it fails and patients die from right heart failure.<sup>3</sup> Abnormalities of the right heart in precPH are not limited to the ventricle but also include the right atrium. Due to diastolic stiffness of the right ventricle, the right atrial (RA) pressure (RAP) increases and RA dilatation is induced.<sup>4</sup> The right atrium is also the location where the ligand bone morphogenetic protein (BMP) 10 is

produced in the adult human heart.<sup>5</sup> BMP10 is one of the circulating ligands, along with BMP9 (mainly produced by the liver),<sup>6,7</sup> able to transduce a signalling by binding to an activin receptor-like kinase 1 (ALK1)/BMP receptor type 2 (BMPR2) complex mainly expressed by endothelial cells. Ligand binding leads to phosphorylation and translocation of SMAD1/5/8 into the nucleus.<sup>8,9</sup> In precPH, there is a known disbalance between BMP and transforming growth factor-beta (TGF- $\beta$ ) signalling, partially caused by loss-of-function mutations in the BMPR2 gene.<sup>10</sup> BMP10 release may be induced to compensate for the BMP/TGF- $\beta$  disbalance. Therefore, it may be hypothesized that increased wall stress due to excessive RA

dilatation or increased RAP may trigger BMP10 secretion. Therefore, it is pivotal to obtain more insights in the role of BMP10 in precPH.

Interestingly, expression levels of BMPs do not necessarily correlate with binding to their receptor complex or level of signalling pathway activation.<sup>11</sup> The activity of BMPs is tightly controlled by positive and negative regulators of the signaling pathway,<sup>9,12</sup> which can interfere with receptor binding, inhibit kinase activity, or affect the phosphorylation of downstream targets (i.e. Smads). This complex regulation makes it challenging to establish a direct correlation between BMP levels and downstream transcriptional activity. To date, no information is available on BMP10 activity in the right atrium, right ventricle, and blood of precPH patients. Therefore, this study aims to: (i) determine whether BMP10 expression and transcriptional activity are altered locally in RA tissue or in the circulation and (ii) investigate the association of circulating BMP10 transcriptional activity with RA morphology, function, and disease severity.

## 2. Methods

More information is provided in the [supplementary material](#).

### 2.1 Study design

This is a prospective cross-sectional study (see [Supplementary material online, Figure S1](#)) of precPH patients: idiopathic pulmonary arterial hypertension (iPAH), hereditary pulmonary arterial hypertension (hPAH), and chronic thromboembolic pulmonary hypertension (CTEPH) diagnosed according to recent guidelines<sup>13,14</sup> at Amsterdam University Medical Center between 22 August 2017 and 02 June 2020. We included healthy controls (without pulmonary or cardiovascular comorbidities). Approval was obtained from the Medical Ethics Review Committee of Amsterdam University Medical Center (NL60827.029.17-PERSEPHONE, 2017.318-DOLPHIN). Informed written consent was obtained from all subjects, and the investigation conformed according to the principles outlined in the Declaration of Helsinki.

We prospectively included 48 precPH patients ( $n = 22$  iPAH, 14 hPAH, and 12 CTEPH; [Supplementary material online, Table S1](#)) and 16 controls, from which we measured BMP10 plasma levels and transcriptional activity. In a subset, we also collected RA blood samples ( $n = 37$  precPH patients and 11 controls) to check BMP10 plasma levels directly in the right atrium and validate the systemic measurements. In another cohort of CTEPH patients ( $n = 13$ ), BMP10 transcriptional activity was measured at baseline and 6 months after pulmonary endarterectomy (PEA).

Exclusion criteria were pregnancy, claustrophobia, or a pacemaker. We also included controls ( $n = 16$ ) that were matched on age and gender to patients. Exclusion criteria for controls included diagnosis of pulmonary hypertension (PH) according to ERS and ESC guidelines,<sup>13,14</sup> an increased pulmonary artery wedge pressure (PAWP > 15 mmHg), tricuspid valve dysfunction, right ventricular (RV) dysfunction, a dilated right atrium or RA dysfunction (related to atrial fibrillation or congenital abnormalities and previous cardiac surgery), and age < 18 years.

### 2.2 RA tissue collection

We prospectively obtained fresh RA tissue from CTEPH patients undergoing PEA and controls undergoing cardiothoracic surgery (coronary artery bypass grafting or aortic valve replacement) to study BMP10 gene expression using quantitative real-time polymerase chain reaction (RT-PCR). Control subjects were only included in the study if they did not have signs of RV/RA dysfunction, dilatation, or tricuspid regurgitation (TR) on echocardiography. Peri-operative CTEPH patients and controls underwent cardiopulmonary bypass, during which a minute incision was made in the right atrium, from which a small portion of tissue was obtained. The tissue was kept on ice before snap-freezing and subsequent storage in liquid nitrogen. Due to limited RA fresh tissue availability, we also obtained paraffin-embedded RA tissue from deceased control subjects ( $n = 6$ ) and deceased or transplanted end-stage disease precPH patients [ $n = 4$

pulmonary arterial hypertension (PAH)] to study BMP10 protein expression and activity using histological analyses.

### 2.3 Quantitative RT-PCR

Total RNA was extracted from fresh RA tissue from precPH patients ( $n = 5$  CTEPH) and controls ( $n = 9$ ) using Direct-zol RNA Miniprep kit (Zymo Research, United States of America) following manufacturer's protocol and further treated with the DNase I set (Zymo Research). The concentration and purity of the RNA was measured on a Nanodrop One spectrophotometer (Thermofisher Scientific, United States of America). Only samples with good quality and purity were used (ratio A260/A280~2 and ratio A260/A230 > 1.7). Reverse transcription to cDNA was carried out using the iScript™ cDNA Synthesis Kit (Bio-Rad, United States of America). Quantitative RT-PCR amplifications were performed with 2  $\mu$ L cDNA in a final volume of 10  $\mu$ L, containing 5  $\mu$ L Fast SYBR Green MasterMix (Thermofisher Scientific), 2  $\mu$ L RNase-free PCR-grade water (Thermofisher Scientific), and 1  $\mu$ L of both forward and reverse primers solution (sequences are specified in [Supplementary material online, Table S2](#)). Hypoxanthine guanine phosphoribosyltransferase (HPRT) was the housekeeping gene used to ensure the validity and reproducibility of the results. Data were collected and analysed in duplicate on the CFX384™ Real-Time System (C1000 Touch™ Thermal Cycler, Bio-Rad). The Livak method<sup>15</sup> was used to quantify the relative ( $2^{-\Delta\Delta C_t}$ ) expression of each gene compared with the housekeeping gene on both precPH and control groups.

### 2.4 Immunohistofluorescent staining

RA paraffin-embedded tissue from controls ( $n = 6$ ) and precPH patients ( $n = 4$  PAH) was stained using an antibody against BMP10 (diluted 1:200; Biorbyt, United Kingdom), cardiac Troponin T (cTnT, diluted 1:500; Abcam, United Kingdom), phosphorylated receptor-regulated Smad1, Smad5, and Smad8 (pSMAD1/5/8, diluted 1:200; Cell Signaling, United States of America), and inhibitor of differentiation 3 (ID3, diluted 1:50; Santa Cruz Biotechnologies, United States of America). The sections were treated with 0.1% sudan black for 30 min at room temperature and counterstained with Hoechst 33342 nuclear dye (diluted 1:500; Santa Cruz Biotechnology) and rhodamine Ulex europaeus agglutinin I (Ulex, diluted 1:200; Vectorlabs, United States of America). Images were captured at  $\times 20$  and  $\times 60$  magnifications under a laser confocal microscope (Nikon A1R) after establishing the right settings according to the negative control staining. Whole-slide image acquisition was performed on Vectra Polaris (Akoya Biosciences, United States of America) at  $\times 10$ ,  $\times 20$ , and  $\times 40$  magnifications.

BMP10 quantification on longitudinal myofibres was performed on images acquired on the Vectra Polaris using the same settings and procedure for all patients and processed with inForm® Tissue Analysis Software v. 2.5 (Akoya Biosciences) to remove the tissue autofluorescence before quantification (see [Supplementary material online, Figure S2](#)). The auto-fluorescence removal required a negative control RA tissue incubated only with the specific secondary antibodies and the specific spectral library created for these secondary antibodies on RA tissue. For the quantification, we measured the total area stained positively with BMP10 and corrected by the total area of the tissue and the number of cells (Hoechst positively stained area). Furthermore, the BMP10 immunofluorescence intensity was also measured exclusively on the myocardial tissue by making a mask with the cTnT positive staining, and it was also corrected by the myocardial area (cTnT positively stained area). pSMAD1/5/8 and ID3 quantifications comprised the number of positive nuclei and were performed on images acquired on the confocal microscope after correction for the negative control, which was RA tissue incubated only with the specific secondary antibodies.

Quantitative histological measurements were assessed through ImageJ analysis software (NIH) with at least 10 random fields averaged per patient.

## 2.5 Right heart catheterization

Haemodynamic assessment and post-processing were performed as previously described.<sup>16</sup> Right heart catheterization (RHC) was performed using a balloon-tipped, flow-directed 7.5-Fr triple lumen Swan-Ganz catheter (Edwards Lifesciences LLC, United States of America).

Pressure curves of pulmonary artery pressure (PAP), RAP, and PAWP were recorded and analysed. Cardiac output (CO) measurements were obtained with the thermodilution method. Pulmonary vascular resistance (PVR) was calculated using the following formula: (mean PAP-PAWP)/CO. RAP curves were analysed for minimal pressures and maximal pressures during the A-wave and the V-wave.

## 2.6 Cardiac magnetic resonance imaging

Cardiac magnetic resonance (CMR) scans were made using a Siemens 1.5-T Sonata or Avanto scanner (Siemens Medical Solutions, Germany). CMR imaging was used to determine RA and RV volumes. Acquisition of scans and post-processing was performed as described before.<sup>17</sup>

## 2.7 Plasma and serum samples collection

Venous blood samples from 16 controls and 48 precPH patients (22 iPAH, 14 hPAH, and 12 CTEPH) were processed immediately after withdrawal and maintained at 4°C during the whole procedure. PrecPH patients underwent RHC and CMR <1 year before participation. In a subset ( $n = 48$ : 11 controls, 20 iPAH, 10 hPAH, and 7 CTEPH), RA blood samples were also collected during RHC in addition to the venous blood samples. In another cohort of CTEPH patients ( $n = 13$ ), serum was collected at baseline and 6 months post-PEA. Plasma samples were obtained from whole blood collected into ethylenediaminetetraacetic acid-treated tubes, while serum samples were obtained from untreated tubes. The tubes were centrifuged at 3000 g at 4°C for 15 min without break to remove the cells, and the upper part was collected, aliquoted, and stored at -80°C.

## 2.8 Enzyme-linked immunosorbent assay

Peripheral venous and RA plasma samples from precPH patients and controls were tested with a commercially available kit that has been validated and is specific for the growth factor domain (GFD) of the BMP10 peptide (DY2926, R&D Systems, United States of America), without any cross-reactivity against the BMP10 pro-peptide (aa 20–313). It also does not show cross-reactivity or interference against BMP9 or other BMP ligands. In addition, the samples were also tested on a commercial and validated kit for the BMP9 peptide (DY3209, R&D Systems) ligand following the manufacturer's protocol. Briefly, 96-well plates were coated with the capture antibody overnight at room temperature, washed, blocked for 1 h, incubated with 100 µL of non-diluted sample for 2 h, washed, incubated with the detection antibody for 2 h, washed, and revealed with streptavidin-horseradish peroxidase working solution, and finally optical density was determined using the Epoch Gen5 microplate reader (Biotek, Agilent, United States of America) set at 450 nm with the 540 nm wavelength subtraction. In the sample plate, increasing recombinant BMP9 or BMP10 concentrations were included for the standard curve (0–2000 pg/mL).

## 2.9 BMP-responsive element dual-luciferase activity assay

Human microvascular endothelial cells (HMECs) were cultured in MCDB 131 medium (Merck, Germany) with 10% fetal bovine serum, 10 ng/mL epidermal growth factor, 1 µg/mL hydrocortisone, glutamax (Thermofisher Scientific), and 100 U/mL penicillin/streptomycin in 0.1% gelatine-coated dishes and were used between passages 19 and 25. To generate HMECs-BRE-LUC cells, HMECs were stably transduced with lentiviruses carrying a BMP-responsive element (BRE)-Luciferase reporter.<sup>18</sup> HMECs-BRE-LUC cells were sub-confluently seeded in pre-coated 48-well plates for 24 h. Then, cells were serum starved for 6 h in Dulbecco's Modified Eagle Medium high-glucose medium and incubated

with stimulation [10% of donor-derived venous serum, and ALK1-Fc (0.5 µg/mL), anti-BMP9 (0.5 µg/mL), or vehicle control]. After 30 min of incubation at room temperature, the cell starvation medium was replaced by every particular sample, and the cells were incubated for 16 h prior to cell lysis. Luciferase activity was measured using a Perkin Elmer luminometer Victor3 1420 device following the instructions provided by the luciferase kit manufacturer (Promega, United States of America) and normalized for protein content using the DC Protein Assay kit (Bio-Rad). All experiments were performed in quadruplicates. Optimization of the technique is shown in [Supplementary material online, Figure S3](#).

## 2.10 Statistical analysis

Data are presented as mean [standard deviation (SD)] or median (interquartile range) or standard error of the mean. Normality of data was checked with histograms and Kolmogorov-Smirnov testing. Log transformation or square root transformation was applied to non-normally distributed data. To compare mRNA expression, immunofluorescence quantification, and plasma levels between precPH and controls, an independent sample t-test or Wilcoxon rank-sum test was used. To compare precPH subgroups and controls, a one-way analysis of variance (ANOVA) with Bonferroni-corrected post-hoc pairwise t-testing was applied. To test relationships between two continuous variables, univariate linear regression was used. To compare stratified precPH patients according to RA dilation, RV dilation, RAP, RV ejection function (RVEF), and N-terminal pro b-type natriuretic peptide (NT-proBNP), an independent sample t-test was used: \* $P \leq 0.05$ , \*\* $P \leq 0.01$ , and \*\*\* $P \leq 0.001$  vs. control group (or otherwise indicated).

## 3. Results

Study design is shown in [Figure 1](#). Control and precPH patients' characteristics are shown in [Table 1](#). Half of the patients were treatment naïve, and among those receiving treatment, there were no differences in mono-, combination, or triple therapy regimens. Disease severity was similar across precPH subgroups, shown by similar pulmonary arterial pressure, PVR, RV dimensions, and functions (see [Supplementary material online, Table S1](#)).

### 3.1 Increased BMP10 expression in RA tissue from pre-capillary PH

We first determined the expression of BMP10 mRNA in RA tissue of precPH patients and controls. Due to the limited availability of RA tissue, which is not routinely collected, we used tissue from separate patient cohorts. To ensure RNA integrity, fresh RA tissue samples were collected from CTEPH patients undergoing PEA and controls undergoing cardiac surgery, and BMP10 mRNA expression was analysed. Interestingly, RA tissue from CTEPH patients showed ~2-fold higher BMP10 mRNA levels compared with controls ( $P < 0.05$ , [Figure 2A](#)). Next, we investigated BMP10 protein expression using immunohistofluorescent stainings. For this analysis, we made use of previously collected RA samples of PAH patients who died from right heart failure. Control tissue was obtained from patients who deceased from non-cardiovascular disorders. As can be appreciated, BMP10 protein ([Figure 2D–G](#); see [Supplementary material online, Figure S2C](#)) is located in the myocardium expressed by RA cardiomyocytes (cTnT) and cardiac endothelium (Ulex-rhodamine) of precPH patients and controls with different intensities. In addition, BMP10 fluorescent area and myocardial intensity were significantly higher in RA tissue of precPH patients in comparison with controls ( $P < 0.05$ , [Figure 2B and C](#)).

Upon binding, BMP10-induced receptor activation results in phosphorylation of Smad1/5/8 (pSMAD1/5/8) and subsequent translocation of pSMAD1/5/8 into the nucleus to initiate gene transcription of BMP-specific target genes, such as ID3.<sup>6</sup> To determine BMP10-related transcriptional activity, we therefore stained paraffin-embedded RA tissue for pSMAD1/5/8 and ID3. Both pSMAD1/5/8 and ID3 proteins were localized in the nucleus, and the number of positive nuclei was greater in

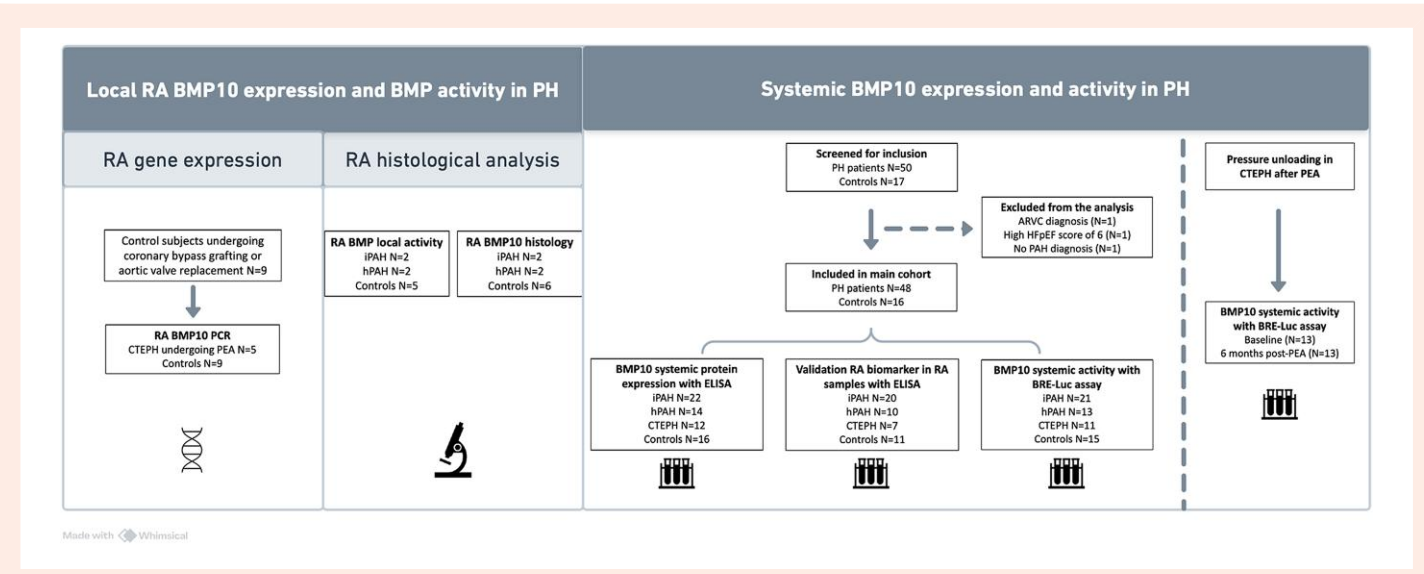


**Figure 1** Study design. Schematic overview of study populations used for each analysis. We studied BMP10 gene expression in fresh RA tissue of five CTEPH from the main cohort undergoing PEA and nine control subjects undergoing coronary bypass or aortic valve replacement. Due to limited fresh RA tissue availability, we also collected post-mortem or transplanted paraffin-embedded RA tissue from PAH patients ( $n = 2$  iPAH and  $2$  hPAH) and from six controls to study BMP10 protein expression and activity using histological analysis. Furthermore, we included 48 pre-capillary PH patients [ $n = 22$  iPAH,  $n = 14$  hPAH ( $n = 12$  BMPR2 mutation carrier and  $n = 2$  GDF2 mutation carrier), and  $n = 12$  CTEPH] and 16 controls, from which we measured circulating BMP10 protein expression and transcriptional activity in peripheral blood samples. In a subset of patients, we also collected RA blood samples ( $n = 37$  PH patients,  $n = 11$  controls) to check BMP10 levels directly in the right atrium.

precPH vs. controls (Figure 3A–D). In addition, pSMAD1/5/8 and ID3 positive nuclei were mostly observed in cardiac endothelial cells (Ulex-positive cells, Figure 3B, C, E, and F), where the ALK1/BMPR2 complex is mainly expressed. Taken together, these findings suggest that both the expression of BMP10 and its signalling activity are increased in RA tissue of precPH patients.

### 3.2 BMP10 protein and transcriptional activity in systemic circulation

Next, we determined if the increased expression of BMP10 in RA tissue of precPH patients resulted in increased secretion of BMP10 ligand into the systemic circulation. For this purpose, we used an enzyme-linked immunosorbent assay (ELISA) kit specific for the detection of BMP10 GDF and analysed peripheral plasma samples prospectively obtained during RHC from 48 precPH patients [ $n = 22$  iPAH,  $n = 14$  hPAH of which  $n = 12$  BMPR2 and  $n = 2$  GDF2 (growth differentiation factor 2, encoding BMP9) mutation carriers, and  $n = 12$  CTEPH patients] and 16 healthy controls. BMP10 protein plasma levels were significantly higher in precPH patients compared with controls (Figure 4A). Subgroup analyses revealed that BMP10 levels were significantly increased in iPAH and CTEPH, with a trend for hPAH (Figure 4B). In addition, we also observed a significant increase in BMP9 protein plasma levels in precPH, which was lost in the subgroups (Figure 4C and D), and a moderate correlation between BMP10 and BMP9 circulating levels (Figure 4E and F). Next, we performed an ELISA in a subset of blood samples obtained during RHC at the RA location ( $n = 37$  precPH patients and  $n = 11$  controls). Interestingly, we observed that the RA BMP10 protein levels strongly correlated to peripheral venous BMP10 protein levels ( $R^2 = 0.93$ ,  $P < 0.0001$ ; see *Supplementary material online*, Figure S3), suggesting that there is no need to collect RA samples during RHC. Therefore, BMP10 protein levels can potentially be assessed using peripheral venous blood samples.

Activity of the BMP signalling pathway is controlled by circulating coactivators and antagonists.<sup>12,19</sup> It is therefore pivotal to not only assess BMP10 protein plasma levels but also determine the BMP10 transcriptional activity in plasma to understand and appreciate BMP10 signalling and

activation capacity. Therefore, we made use of a previously validated BMP10 activity assay using a genetically modified human microvascular endothelial cells (HMECs) line with a BMP-responsive promoter driving the expression of the firefly luciferase reporter gene (BRE-LUC).<sup>18</sup> We exposed the HMECs-BRE-LUC to 10% patient- or control-derived serum. To discriminate the BRE-LUC activity induced by BMP10 from the one resulting from other BMP ligands present in the serum, we used two pharmacological tools<sup>20</sup>: a BMP9-specific antibody (anti-BMP9) to capture BMP9 and a Fc-fused soluble ALK1 extracellular domain (ALK1-Fc) to sequester both BMP9 and BMP10 (Figure 5A; *Supplementary material online*, Figure S4). BMP10-induced transcriptional activity is calculated as the induced promoter activity difference between the anti-BMP9 and ALK1-Fc treatments. As shown in Figure 5B, pre-incubation with anti-BMP9 reduced baseline activity (shown as 100%), which was further decreased by BMP9 and BMP10 sequestration using ALK1-Fc. When comparing the precPH subgroups with controls, we observed no differences in the BMP10-induced transcriptional activity (Figure 5C). Taken together, these data demonstrate increased circulating levels of BMP10 in plasma of precPH patients in comparison with controls, while no alterations were observed in BMP10 transcriptional activity.

### 3.3 Potential triggers of increased BMP10 secretion

To understand what triggers the increase in circulating BMP10 protein and activity, we determined its association with RA and RV dilatation, pressure, and function. RA and RV dilatation was defined based on previously published normal values of RA and RV dimensions (RA dilatation was defined as maximal RA volume  $>79$  mL/mm $^2$  for male patients or  $>69$  mL/mm $^2$  for female patients; RV dilatation was defined as RV end-diastolic volume index  $\geq 109$  mL/mm $^2$  for males and  $\geq 97$  mL/mm $^2$  for females).<sup>21</sup> Interestingly, RA dilatation was associated with significantly higher BMP10 activity, while no change was observed with RV dilatation or circulating BMP10 protein levels (Figure 6). In addition, we also studied cardiac pressure and function using the well-established and validated cut-off values for NT-proBNP, RAP, and RVEF. In patients with high NT-proBNP levels ( $>1100$  ng/L)<sup>22</sup>

**Table 1** Baseline characteristics of subjects included in the study

	Control	PrecPH	P-value
N	16	48	
Age, years (SD)	50 (14)	51 (14)	0.80
Sex = female, n (%)	9 (56)	32 (67)	0.65
BMI, kg/m <sup>2</sup> (SD)	26 (4)	27 (5)	0.77
NYHA (%)			<b>&lt;0.001</b>
NYHA I	15 (94)	4 (8)	
NYHA II	1 (6)	23 (48)	
NYHA III	0 (0)	19 (40)	
NYHA IV	0 (0)	2 (4)	
6MWD, m (SD)	NA	457 (119)	NA
NT-proBNP, pg/mL (IQR)	23 (9–62)	459 (195–1664)	<b>&lt;0.001</b>
eGFR, mL/min/1.73 m <sup>2</sup> (SD)	78 (13)	72 (18)	0.45
Diuretics use, n (%)	1 (6)	25 (52)	<b>0.003</b>
PH-specific drugs (%)			<b>0.001</b>
Treatment naïve	16 (100)	21 (44)	
Mono therapy	0 (0)	6 (13)	
Combination therapy	0 (0)	12 (25)	
Triple therapy	0 (0)	9 (19)	
Smoking, n (%)			0.74
Non-smoking	2 (33)	17 (44)	
Former smoker	3 (50)	19 (49)	
Current smoker	1 (17)	3 (8)	
Coronary artery disease, n (%)	0 (0)	1 (2)	1
Hypertension, n (%)	1 (6)	11 (23)	0.27
Diabetes, n (%)	0 (0)	3 (6)	0.73
RHC			
Heart rate, bpm (SD)	74 (13)	99 (161)	0.62
Systolic BP, mmHg (SD)	127 (19)	122 (19)	0.37
Diastolic BP, mmHg (SD)	82 (16)	79 (14)	0.45
Mean PAP, mmHg (SD)	19 (3)	51 (17)	<b>&lt;0.001</b>
Mean RAP, mmHg (SD)	6 (5–7)	8 (5–10)	<b>0.03</b>
PCWP, mmHg (SD)	11 (3)	11 (3)	0.84
Cardiac index, L/m <sup>2</sup> (SD)	3.0 (0.7)	2.5 (0.7)	0.06
SVO <sub>2</sub> , % (SD)	74 (4)	64 (11)	<b>0.003</b>
PVR, WU (IQR)	1.3 (1.2–1.8)	8.2 (5.9–12.5)	<b>&lt;0.001</b>
CMR			
RVEDVi, mL/m <sup>2</sup> (SD)	65 (13)	99 (25)	<b>&lt;0.001</b>
RVESVi, mL/m <sup>2</sup> (SD)	27 (9)	61 (26)	<b>&lt;0.001</b>
RVEF, % (SD)	59 (6)	40 (15)	<b>&lt;0.001</b>
SVi, mL/m <sup>2</sup> (SD)	41 (7)	40 (11)	0.73

Normality of data was checked. Statistical differences between precPH patients and controls were tested with an independent sample *t*-test or Wilcoxon rank-sum test. Statistically significant *P*-values in bold.

BMI, body mass index; NYHA, New York Heart Association; 6MWD, 6-min walking distance; eGFR, estimated glomerular filtration rate; IQR, inter-quartile range; BP, blood pressure; NA, not available; RAP, right atrial pressure; PCWP, pulmonary capillary wedge pressure; SVO<sub>2</sub>, mixed venous oxygen saturation; RVEDVi, RV end-diastolic volume index; RVESVi, RV end-systolic volume index; RVEF, RV ejection fraction; SVi, stroke volume index.

and low RVEF (<35%),<sup>17</sup> BMP10 activity levels were significantly higher. No interaction was observed with circulating BMP10 protein levels. Patients with high RAP (>14 mmHg)<sup>22</sup> tended to have increased BMP10 activity (*P* = 0.11). BMP10 transcriptional activity and protein levels in precPH patients were not related to the presence of TR. Moderate TR was present in *n* = 13 patients, which did not show higher BMP10 levels or activity than

patients without TR (*n* = 31) [1.4 vs. 1.3 pg/mL (*P* = 0.78) and 14 vs. 18% (*P* = 0.48), respectively]. Table 2 shows all relations of clinical values with high BMP10 activity.

Furthermore, to investigate the effect of pressure unloading on BMP10 activity, we also measured BMP10-induced transcriptional activity in a small group of CTEPH patients at baseline and post-PEA (Figure 7A). BMP10-induced transcriptional activity was significantly reduced after the intervention which coincided with improvements in disease severity, haemodynamics, and RV function (*P* < 0.05, Figure 7B; Supplementary material online, Table S4).

Taken together, these results indicate a close association between RA remodelling, pressure overload, and BMP10 transcriptional activity. Further studies are needed to determine whether elevated BMP10 transcriptional activity represents a maladaptive response mechanism or should be targeted selectively for therapeutic intervention.

## 4. Discussion

In this study, we combined investigations of BMP expression and signalling in RA tissue and blood samples of precPH patients with sophisticated assessment of RA morphology, function, and disease severity parameters. In summary, we demonstrated the following:

- (1) BMP10 expression and downstream transcriptional activity in RA tissue from precPH patients is increased.
- (2) BMP10 plasma levels are increased, while BMP10 activity is preserved, in precPH.
- (3) RA dilatation, but not RV dilatation, is closely associated with high BMP10 activity, as well as high NT-proBNP and low RV ejection fraction.
- (4) Pressure unloading results in reduced BMP10 transcriptional activity in CTEPH patients.

### 4.1 RA BMP10

To date, over 300 mutations have been identified in the *BMPR2* gene in PAH, underscoring the importance of disturbed BMP signalling in the disease.<sup>23</sup> Only recently, mutations in the *BMP10* gene have been identified in familial PAH.<sup>23</sup> BMP10 can bind to ALK1, ALK3, and ALK6 in a complex with BMPR2, with high affinity for the ALK1/BMPR2 receptor complex.<sup>6,7,24</sup> The ALK1/BMPR2 complex is specifically expressed on vascular endothelial cells, while the low-affinity ALK3 and ALK6 receptors are located on diverse cell types, such as cardiomyocytes.<sup>19</sup> In adulthood, BMP10 is almost exclusively produced and secreted into the extracellular space by RA cardiomyocytes and can signal in autocrine and paracrine manners mainly by binding to vascular receptors.<sup>19,25</sup> In line with this, our stainings confirmed BMP10 presence on both cardiomyocytes and vascular cells in the RA tissue.

The effect of BMP10 on the ventricle has not been studied in detail, but increased BMP10 expression was observed in hypertrophied left ventricles of hypertensive rats.<sup>26</sup> While never investigated, BMP10 may play an important role in cardiac adaptation in precPH, given its crucial function in cardiovascular development and maintenance. Furthermore, BMP10 is almost exclusively expressed in the adult right atrium,<sup>27</sup> suggesting a tissue-specific role that remains elusive. For the first time, we could reveal that RA dilatation is closely associated with high BMP10 activity. As a consequence of RV diastolic stiffness, the RA has to cope with an increased pressure overload. Recent results have revealed RA ventricular uncoupling in patients with precPH characterized by excessive RA dilation and increased RA pressure.<sup>4</sup> We therefore hypothesize that the increased RA dilation results in increased wall stress on the RA cardiomyocytes triggering BMP10 secretion. It is known that RA cardiomyocytes secrete different peptides and several inflammatory cytokines under stretch.<sup>28</sup> In fact, several BMP10 and BMP9 downstream genes (i.e. *SMAD6*, *SMAD7*, and *ENDOTHELIN-1*) have been described as mechano-responsive genes.<sup>29</sup> Finally, histological analyses have revealed that BMP10 co-localizes with T-cap, a key mechano-sensory protein, in cardiomyocytes. These data

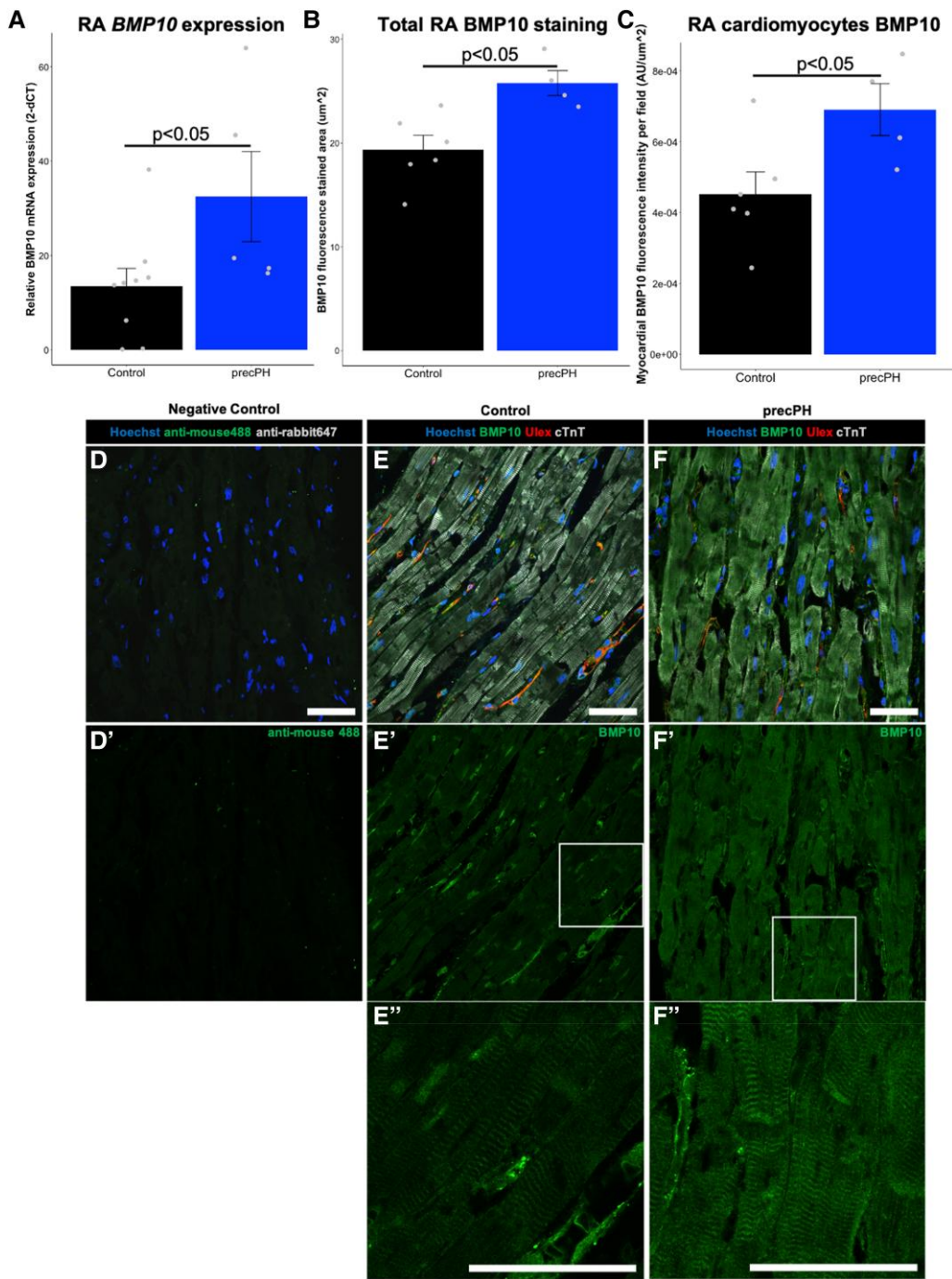


**Figure 2** Up-regulated local BMP10 expression in the right atrium of precPH patients. (A) Quantification of the relative BMP10 mRNA expression in control ( $n = 9$ ) and precPH ( $n = 5$  CTEPH) RA tissues. (B and C) Quantification of total RA BMP10 fluorescent area and RA cardiomyocytes BMP10 intensity levels in control ( $n = 6$ ) and precPH ( $n = 4$  PAH) paraffin-embedded RA tissue sections stained against BMP10, respectively. Representative immunofluorescent stainings of BMP10, Ulex-rhodamine (Ulex, endothelium), and cardiac TroponinT (cTnT, myocardium) in the negative control sample for anti-rabbit Alexa488 and anti-mouse Alexa647 (D), in the control (E), and in the precPH (F) RA tissues at 60 $\times$ -oil magnification. (D'–F') Alexa488 single-channel images from the stainings in (D–F). (E'' and F'') Zoom-in images from (E' and F') to appreciate the sarcomeric pattern of the BMP10 staining in the cardiomyocytes and the homogeneous staining in the vessels. Scale bars = 50  $\mu$ m. Brightness and contrast for the Alexa488 channel have not been modified. Normality of data was checked and transformed if needed, and statistical differences between precPH patients and controls were tested using an independent sample t-test.

suggest a direct link between cardiomyocyte stretch and BMP10 secretion. Unfortunately, due to experimental limitations, we were unable to demonstrate a direct relation between RA stretch and BMP10 release. RA cardiomyocyte stretch experiments<sup>30</sup> were not possible because isolation of

RA cardiomyocytes is challenging, and their lifespan is limited.<sup>31</sup> In addition, commercial atrial cardiomyocyte cell lines do not express BMP10. Therefore, we focused our analyses on RA tissue samples and blood analyses obtained from precPH patients. We were able to demonstrate for

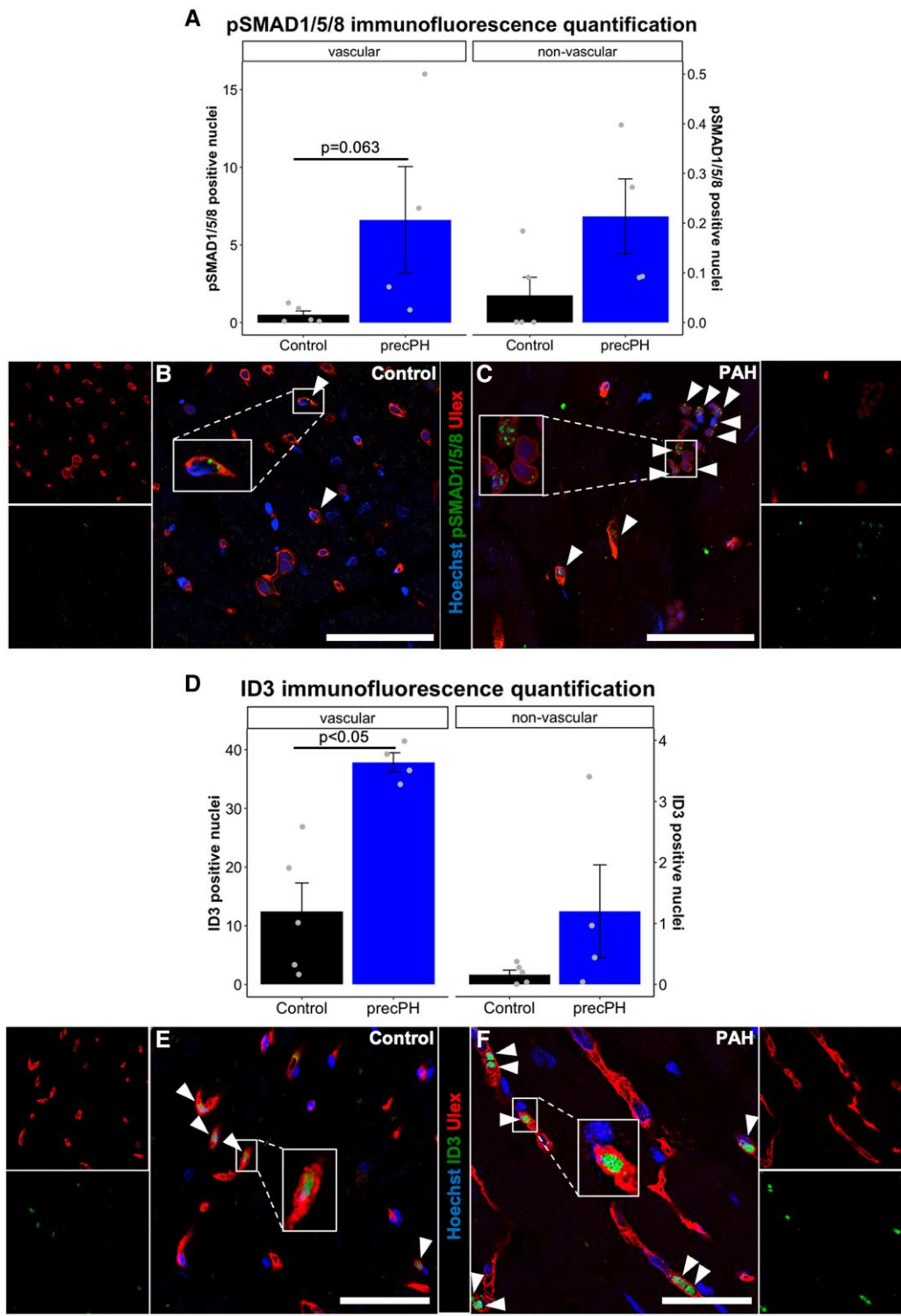


**Figure 3** Up-regulated local BMP10 activity in the right atrium of precPH patients. (A) Quantification of positive pSMAD1/5/8 nuclei in vascular and non-vascular cells within the RA tissues from precPH ( $n = 4$  PAH) and controls ( $n = 5$ ). (B and C) Representative immunofluorescent staining of positive pSMAD1/5/8 nuclei in vascular and non-vascular cells from control and precPH with rhodamine and Alexa488 single-channel images on the sides. (D) Quantification of positive ID3 nuclei in vascular and non-vascular cells within the RA tissues from precPH ( $n = 4$  PAH) and controls ( $n = 5$ ). (E and F) Representative immunofluorescent staining of positive ID3 nuclei in vascular and non-vascular cells from control and precPH with rhodamine and Alexa488 single-channel images on the sides. Arrowheads indicate positive pSMAD1/5/8 and ID3 nuclei. Zoom-in images are included within (B, C, E, and F). Nuclei were counterstained with Hoechst 33342 and vessels with Ulex-rhodamine (B, C, E, and F). Negative control images are shown in [Supplementary material online, Figure S2A](#). Scale bars = 50  $\mu$ m. Vascular and non-vascular measurements are plotted with their own Y-axis on the left or right side, respectively. Normality of data was checked and transformed if needed, and statistical differences between precPH patients and controls were tested using a Wilcoxon rank-sum test (in A and D).

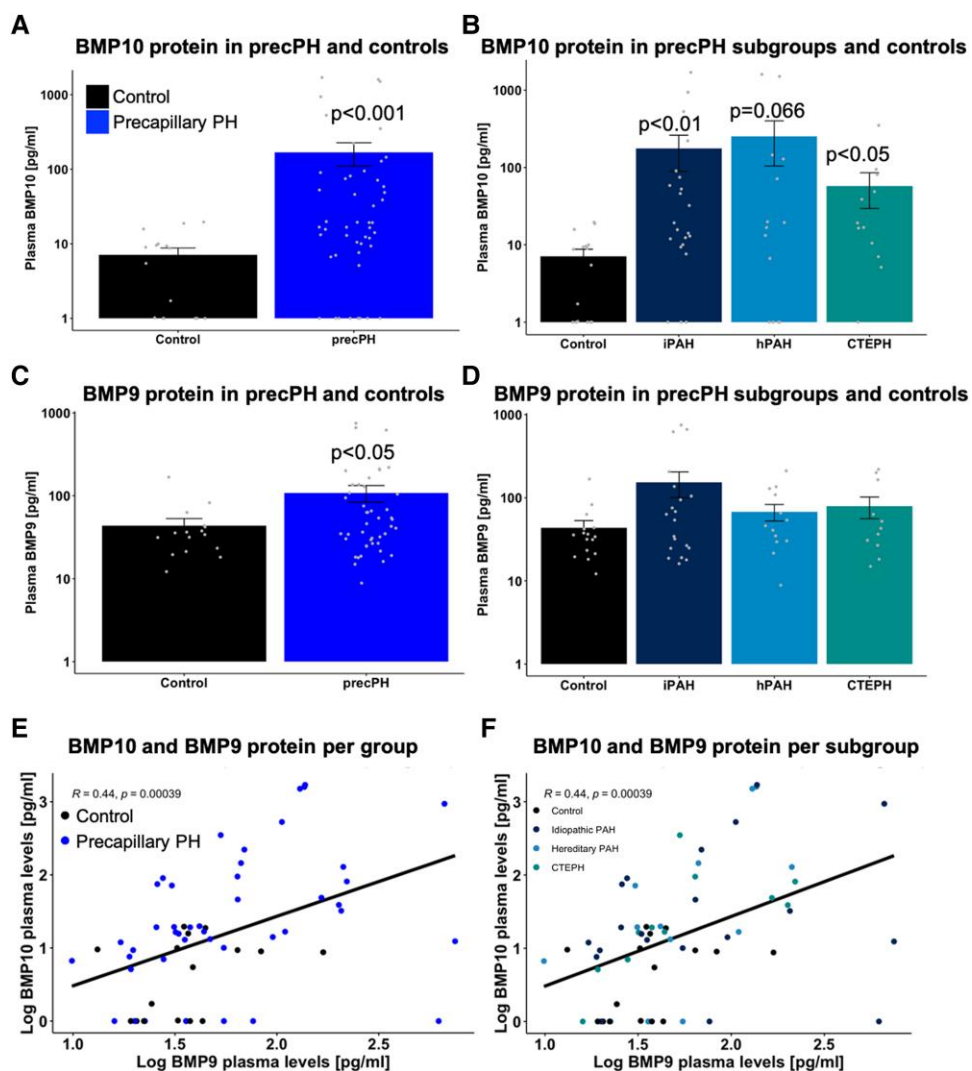


**Figure 4** Higher BMP10 plasma levels in precPH patients compared with controls. (A and B) BMP10 protein circulating plasma levels in precPH patients ( $n = 48$ ) and subgroups ( $n = 48$ : 22 iPAH, 14 hPAH, and 12 CTEPH), respectively, vs. controls ( $n = 16$ ). (C and D) BMP9 protein circulating plasma levels in precPH patients ( $n = 45$ ) and subgroups ( $n = 45$ : 20 iPAH, 14 hPAH, and 11 CTEPH), respectively, vs. controls ( $n = 16$ ). (E and F) Correlation between BMP10 and BMP9 plasma levels in precPH patients ( $n = 45$ ) or subgroups ( $n = 45$ : 20 iPAH, 14 hPAH, and 11 CTEPH), respectively, vs. controls ( $n = 16$ ). Logarithmic Y-axis is used in graphs (A–D). Data in (A and B) are  $y + 1$  for logarithmic scale transformation. Normality of data was checked and transformed if needed. Statistical differences between precPH patients or precPH subgroups and controls were tested with an independent sample t-test or a one-way ANOVA, respectively. Associations were tested with univariate linear regression analysis.

the first time that BMP10 expression and downstream activity in human PH pressure overload RA tissues is significantly increased. Finally, we could show that in CTEPH patients undergoing PEA, improving RV function and haemodynamics coincided with a drop in BMP10 transcriptional activity. How BMP10 expression and activity is regulated is currently unknown and is subject of future experiments.

#### 4.2 Circulating BMP10 in pre-capillary PH and its clinical relevance

Reduced BMP9 and BMP10 plasma levels have been associated with homozygous and heterozygous mutations in the *GDF2* and *BMP10* genes, respectively, in patients with porto-pulmonary hypertension, hepato-pulmonary syndrome, hereditary haemorrhagic telangiectasia, or PAH.<sup>32–34</sup> Early increases in BMP10 levels in preterm infants were strongly

related to development of PH associated with bronchopulmonary dysplasia.<sup>35</sup>

Hodgson et al.<sup>20</sup> investigated plasma levels of BMP9 and BMP10 in PAH patients. They could not report a difference in BMP9 levels but observed reduced BMP10 plasma levels in female PAH patients compared with female healthy controls. In contrast, we describe an increase in both BMP10 and BMP9 plasma levels in precPH patients. BMP10 can circulate in different forms (i.e. homodimers of mature or unprocessed propeptide<sup>20</sup> and BMP9-BMP10 heterodimers have been proposed<sup>36</sup>), and conflicting reports have been published on inactive or active forms of circulating BMP10.<sup>5,37,38</sup> In fact, BMP9 and BMP10 are first produced as a preproprotein with three domains (S-domain, prodomain, and GDF) before being secreted into proprotein (prodomain and GDF), which dimerizes (proBMP9 or proBMP10), and can be further processed into either the folded proprotein complex or cleaved by furin convertases

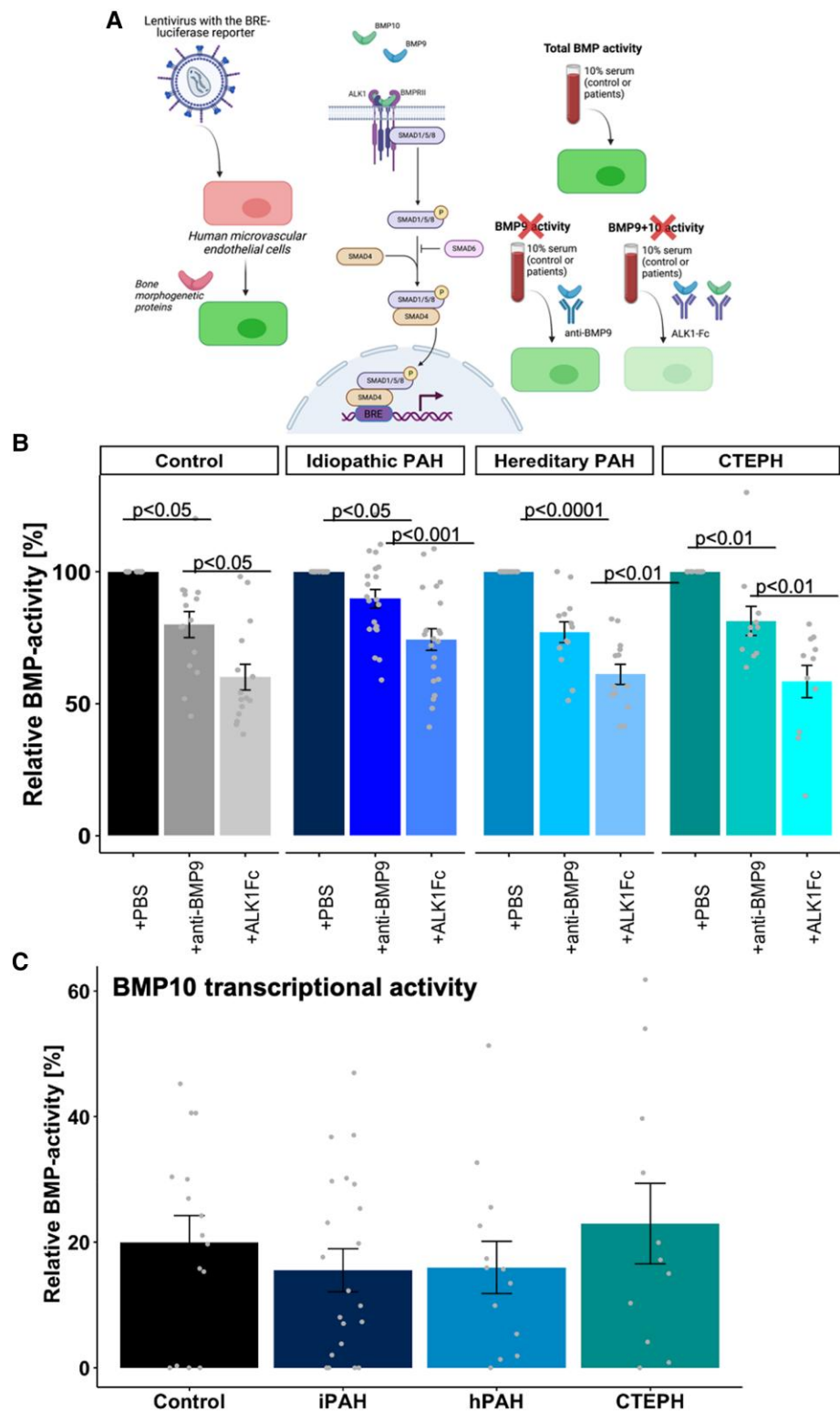


**Figure 5** BMP10 transcriptional activity in precPH patients and controls. (A) Schematic explanation of the BRE-LUC reporter assay to determine BMP transcriptional activity in venous serum. Specific trap antibodies targeting BMP9 or BMP9 and BMP10 are used to assess BMP10 activity. Created with BioRender.com. (B) Relative BMP transcriptional activity as a luciferase read-out from the HMEC-BRE-LUC, endothelial cells expressing a BMP-specific luciferase reporter, in control ( $n = 15$ ) and precPH subgroups ( $n = 21$  iPAH,  $n = 13$  hPAH, and  $n = 11$  CTEPH) after incubation with phosphate-buffered saline (PBS) (baseline), anti-BMP9, or ALK1-Fc (inhibition of BMP9 and BMP10). (C) BMP10 activity in controls and precPH subgroups has been calculated from the subtraction of anti-BMP9 and ALK1-Fc to total BMP activity. Normality of data was checked and transformed if needed. Statistical differences between precPH patients and controls, and between baseline conditions and trap antibodies, were tested with an independent sample *t*-test or a one-way ANOVA, after which pairwise *t*-testing with Bonferroni correction was applied, respectively.

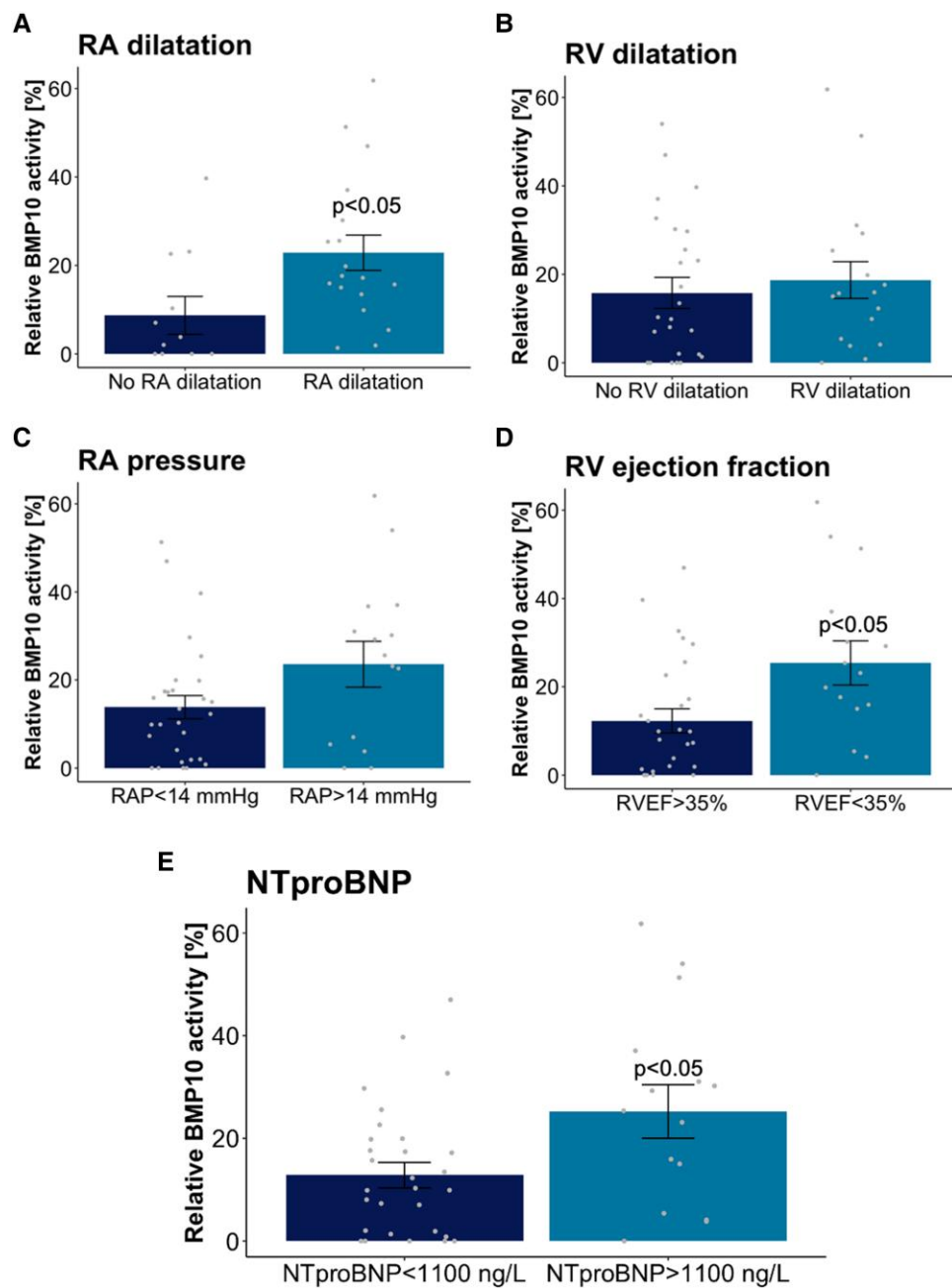


**Figure 6** Patients with more right atrial dilatation, reduced RV ejection fraction, and higher NT-proBNP have higher levels of circulation BMP10 activity. (A and B) BMP10 transcriptional activity in precPH patients with RA or RV dilation, respectively. (C-E) BMP10 transcriptional activity in precPH patients with high RAP, reduced RVEF, or high NT-proBNP, respectively. PrecPH patients were stratified according to RA volume ( $>79 \text{ mL/mm}^2$  for male patients or  $>69 \text{ mL/mm}^2$  for female patients), RV end-diastolic volume index ( $\geq 109 \text{ mL/mm}^2$  for males, and  $\geq 97 \text{ mL/mm}^2$  for females), RAP ( $>14 \text{ mmHg}$ ), RVEF ( $<35\%$ ), and NT-proBNP levels ( $>1100 \text{ ng/L}$ ). Normality of data was checked and transformed if needed. Statistical differences between both groups were tested with an independent samples t-test.

into the GFD dimer or monomer forms (BMP9 or BMP10) and the free prodomain.<sup>20</sup> We used a previously reported commercially available ELISA kit, which detects the GFD of both proBMP10 (immature BMP10) and BMP10 peptides (mature BMP10), unlike other studies directed only towards the unprocessed proBMP10<sup>20</sup>. The mature form can bind to ALK1/BMPR2, whether it is still associated with its prodomain after maturation or not,<sup>20,36</sup> and their ability to activate the BMP signalling pathway in a cell is influenced by a number of factors. The presence of the membrane-

bound or soluble forms of endoglin,<sup>11</sup> activation of the TGF- $\beta$ -SMAD2/3 signalling pathway, plasma levels of agonists/antagonists, or pro-inflammatory cytokines,<sup>39</sup> among others, can influence the subsequent BMP transcriptional activity. It is therefore essential to also measure BMP10 transcriptional activity in addition to BMP10 protein plasma levels as they can differ. To determine BMP10 transcriptional activity in serum samples of precPH patients, we used a BRE-LUC assay that has been validated previously in endothelial cells. Endothelial cells are exposed to 10%

**Table 2** Associations between BMP10 transcriptional activity and clinical characteristics within precPH patients

	Low BMP10 activity	High BMP10 activity	P-value
Number of patients	23	24	
General patient characteristics			
Age [mean (SD)]	48.65 (13.20)	51.50 (15.85)	0.508
Females (%)	14 (60.9)	19 (79.2)	0.293
Diagnoses (%)			0.613
iPAH	12 (52.2)	10 (41.7)	
hPAH	7 (30.4)	7 (29.2)	
CTEPH	4 (17.4)	7 (29.2)	
BMI, kg/m <sup>2</sup> [mean (SD)]	26.17 (5.82)	26.72 (3.76)	0.699
NYHA (%)			0.923
NYHA I	2 (8.7)	1 (4.2)	
NYHA II	11 (47.8)	13 (54.2)	
NYHA III	9 (39.1)	9 (37.5)	
NYHA IV	1 (4.3)	1 (4.2)	
6MWD, m [mean (SD)]	471.31 (110.62)	441.63 (122.06)	0.489
eGFR, mL/min/1.73 m <sup>2</sup> [mean (SD)]	72.69 (18.01)	71.67 (19.52)	0.909
PH-specific drugs (%)			0.514
Treatment naive	9 (39.1)	11 (45.8)	
Mono therapy	2 (8.7)	4 (16.7)	
Double therapy	8 (34.8)	4 (16.7)	
Triple therapy	4 (17.4)	5 (20.8)	
COMPERA risk score			0.247
Low	12 (52.2)	7 (29.2)	
Intermediate	9 (39.1)	15 (62.5)	
High	2 (8.7)	2 (8.3)	
Haemodynamic data			
HR, beats/min [mean (SD)]	72.96 (13.30)	124.71 (226.03)	0.279
mPAP, mmHg [mean (SD)]	49.35 (20.73)	54.96 (13.72)	0.278
mRAP, mmHg [mean (SD)]	7.74 (4.69)	9.67 (5.43)	0.200
PCWP, mmHg [mean (SD)]	10.22 (2.98)	11.26 (2.91)	0.236
Cl, L/m <sup>2</sup> [mean (SD)]	2.70 (0.68)	2.36 (0.70)	0.101
SVO <sub>2</sub> , % [mean (SD)]	66.78 (10.51)	61.39 (10.52)	0.089
PVR, WU [median (IQR)]	6.60 (4.86–11.62)	10.57 (7.81–13.77)	0.057
RV function and adaptation			
NT-proBNP, pg/mL [median (IQR)]	212.00 (108.50–671.00)	835.00 (405.00–2381.00)	<b>0.004</b>
RVEDVi, mL/m <sup>2</sup> [mean (SD)]	94.91 (21.21)	101.48 (29.07)	0.400
RVESVi, mL/m <sup>2</sup> [mean (SD)]	53.32 (23.35)	68.63 (28.04)	0.058
RVEF, % [mean (SD)]	45.91 (12.38)	34.71 (15.04)	<b>0.011</b>
LVSVi, mL/m <sup>2</sup> [mean (SD)]	42.74 (10.39)	35.69 (10.32)	<b>0.031</b>
RA function			
RAP <sub>A-wave</sub> , mmHg [mean (SD)]	13.86 (5.14)	17.83 (8.09)	0.084
RAP <sub>V-wave</sub> , mmHg [mean (SD)]	10.52 (5.47)	13.12 (7.78)	0.250
RAP <sub>min</sub> , mmHg [mean (SD)]	5.51 (4.65)	6.51 (6.26)	0.588
Max RA volume, mL/m <sup>2</sup> [median (IQR)]	84.84 (62.35–134.65)	118.43 (86.62–166.00)	0.076
Diastasis RA volume, mL/m <sup>2</sup> [median (IQR)]	75.80 (53.90–112.25)	108.05 (79.54–146.68)	<b>0.047</b>
Min RA volume, mL/m <sup>2</sup> [median (IQR)]	47.94 (30.60–69.67)	66.99 (47.19–120.73)	0.053
RA longitudinal strain [mean (SD)]	−16.89 (4.71)	−13.77 (5.14)	0.065
Total RAEF, % [mean (SD)]	46.18 (11.01)	38.41 (11.04)	<b>0.032</b>
Active RAEF, % [mean (SD)]	33.64 (14.10)	31.02 (12.42)	0.535
Passive RAEF, % [mean (SD)]	18.14 (9.34)	10.55 (5.05)	<b>0.003</b>
RA stiffness [median (IQR)]	0.12 (0.09–0.13)	0.14 (0.11, 0.18)	0.149

Downloaded from https://academic.oup.com/cardiovascres/article/121/8/1254/8034136 by Jacob Heeren user on 13 February 2026

*Continued*

**Table 2** *Continued*

	Low BMP10 activity	High BMP10 activity	P-value
Minimal RA wall stress [median (IQR)]	24.50 (16.64–38.53)	31.87 (14.83–57.45)	0.516
Maximal RA wall stress [median (IQR)]	69.34 (48.58–85.59)	81.95 (64.62–113.30)	0.199

Characteristics of precPH patients after stratification into high ( $>0.68$  AU) and low ( $\leq 0.68$  AU) BMP10 transcriptional activity. Normality of data was checked. Statistical differences between low BMP10 activity and high BMP10 activity were tested with an independent sample t-test or Wilcoxon rank-sum test. Statistically significant P-values in bold.

BMI, body mass index; NYHA, New York Heart Association; 6MWD, 6-min walking distance; eGFR, estimated glomerular filtration rate; PH, pulmonary hypertension; HR, heart rate; IQR, inter-quartile range; mPAP, mean pulmonary arterial pressure; mRAP, mean right atrial pressure; PCWP, pulmonary capillary wedge pressure; CI, cardiac index;  $\text{SVO}_2$ , mixed venous oxygen saturation; RVEDVi, RV end-diastolic volume index; RVESVi, RV end-systolic volume index; RVEF, RV ejection fraction; SVi, stroke volume index; LVSVi, left ventricular stroke volume index; RAEF, right atrial ejection fraction.

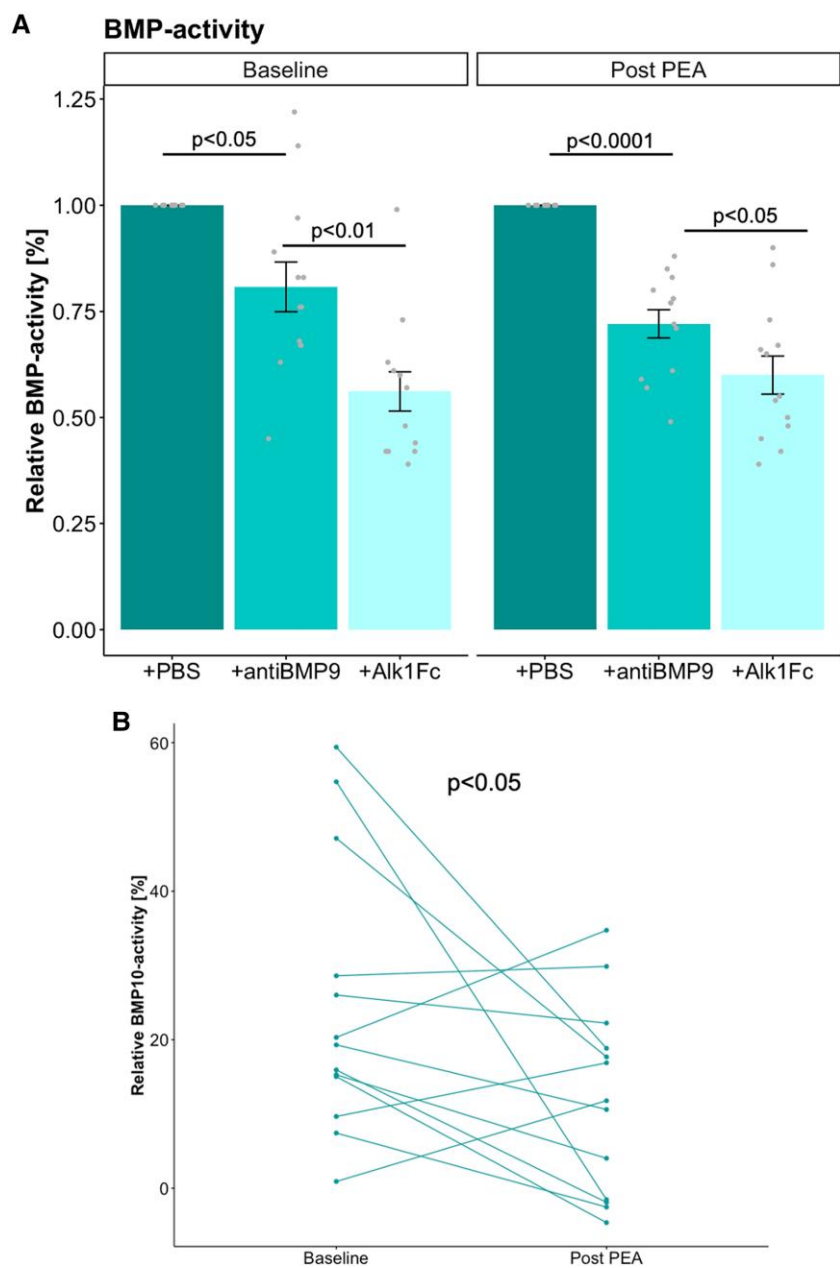


**Figure 7** Effect of pressure unloading on BMP10 activity in precPH patients. (A) Serum relative BMP activity at baseline and post-PEA in CTEPH patients. Incubation with anti-BMP9 only blocked BMP9 activity, while ALK1-Fc blocked both BMP9 and BMP10 activities. (B) Calculated BMP10 transcriptional activity at baseline and post-PEA ( $n = 13$ ), respectively. BMP10 transcriptional activity is calculated by subtracting BMP activity values after incubation with the trap antibodies. Normality of data was checked and transformed if needed. Statistical differences between baseline conditions and trap antibodies, and between baseline and post-PEA, were tested with an independent sample t-test.

serum, and by using specific trap antibodies targeting either BMP9 or BMP9 and BMP10, the transcriptional BMP10 activity can be deducted. Intriguingly, although we did observe a significant increase in circulating BMP10 levels between precPH patients and healthy controls, correlations with clinical parameters of RA dilatation and RV function were only observed with BMP10 transcriptional activity. Suggesting that quantifying BMP10 transcriptional activity has important additional clinical value that is missed when only performing BMP10 ELISA to quantify circulating BMP10 plasma levels. In addition, it is important to realize that different types of BMP10 ELISA exist, each targeting different domains of BMP10. Although measuring BMP10 protein levels is getting more clinical attention in other cardiovascular diseases (such as atrial fibrillation),<sup>40,41</sup> before implementation of BMP10 as clinical biomarker of right heart failure, it should be determined which read-out of BMP10 is most sensitive to predict right heart failure in a large cohort of precPH patients.

### 4.3 Limitations

This was a single-centre study, samples were obtained prospectively, explaining the relatively small sample size and limiting statistical analysis to correct for confounders. Due to limited access to RA tissue of precPH patients, there was heterogeneity in the source of the tissue: (i) we collected fresh RA tissue from CTEPH patients undergoing PEA and (ii) we obtained paraffin-embedded end-stage RA tissue from hPAH and iPAH patients from obduction or lung transplantation. Available RA tissue from CTEPH patients was minuscule and sufficient for only one laboratory technique. Finally, we could not determine BMP10 activity directly using trap antibody against BMP10 (#MAB2926, R&D Systems), as described,<sup>20</sup> because this antibody did not inhibit BMP10 transcriptional activity in our samples; therefore, we used the ALK1-Fc.

### Translational Perspective

Our study provides important insights into the role of bone morphogenetic protein 10 (BMP10) in pre-capillary pulmonary hypertension (precPH) at both fundamental and clinical levels. We correlated BMP10 expression and transcriptional activity in right atrial (RA) tissue and systemic circulation with clinical haemodynamics. Our findings demonstrate that precPH patients have increased BMP10 expression and transcriptional activity in the right atrium, along with elevated BMP10 plasma levels. Furthermore, we revealed that BMP10 activity is associated with RA dilatation and can be reduced by pressure unloading, indicating that RA stretch might be involved in BMP10 secretion.

## 5. Conclusions

In this study, we could demonstrate that BMP10 expression and circulating plasma levels are increased in patients with precPH. RA dilatation, reduced RV function, and high levels of NT-proBNP were closely associated with high BMP10 transcriptional activity. Finally, pressure unloading in CTEPH patients resulted in a significant drop of BMP10 transcriptional activity, whereas no change was observed in BMP10 circulating plasma levels. Future studies are needed to identify the triggers of BMP10 secretion, determine the best read-out of BMP10 in the clinical setting, and reveal whether BMP10 is a treatment target or a ligand released upon stretch aimed to enhance cardiac adaptation.

## Supplementary material

Supplementary material is available at *Cardiovascular Research* online.

## Authors' contributions

Substantial contributions to the conception or design of the work (A.L.-V., J.v.W., J.A.G., G.S.-D., M.J.G., F.S.d.M.); or the acquisition (A.L.-V., J.v.W., J.A.G., R.S., C.B., A.K., S.M.A.J., J.N.W., M.L.H., L.J.M., J.T.M., P.S., H.W.M.N.), analysis, or interpretation of data for the work (A.L.-V., J.v.W., G.S.-D., M.J.G., F.S.d.M.) or drafting the work (A.L.-V., J.v.W., J.A.G., G.S.-D., M.J.G., F.S.d.M.) or reviewing it critically for important intellectual content (all authors). Final approval of the version to be published (all authors). Agreement to be accountable for all aspects of the work in ensuring that questions related to the accuracy or integrity of any part of the work are appropriately investigated and resolved (all authors).

## Acknowledgements

We would like to specially thank N. J. Braams and the Pulmonology Department for the inclusion of patients and healthy subjects, as well as X. Pan for the plasma and serum collection. We want to thank Prof. ten Dijke from Leiden University Medical Center for the pGL3-(BRE)2-luciferase plasmid to study BMP activity. We appreciate the help of the

Microcopy and Cytometry Core Facility at Amsterdam UMC during image acquisition.

**Conflict of interest:** M.L.H. reports personal fees from Novartis, Boehringer Ingelheim, Daiichi Sankyo, Vifor Pharma, AstraZeneca, Bayer, MSD, and Quin, outside the submitted work. The other authors report no conflicts.

## Funding

This research was financially supported by the Netherlands Organization for Scientific Research: NWO-VICI no. 918.16.610 (J.A.G and A.V.-N.) and NWO-VIDI no. 917.18.338 (F.S.d.M.). The work was also funded by the Hartstichting Dekker senior post-doc grant no. 2018T059 (J.v.W. and F.S.d.M.) and the Dutch Cardiovascular Alliance: CVON-2017-10 DOLPHIN-GENESIS (A.V.-N., F.S.d.M., H.J.B., and M.J.G.) and CVON-2018-29 PHAEDRA-IMPACT (A.L.-V., C.B., A.V.-N., H.J.B., M.J.G., and F.S.d.M.). G.S.-D. is also sponsored by Fundació La Marató de TV3 (#202038) and the Ministerio de Ciencia e Innovación through the Ramón y Cajal grant (#RYC2021-030886-I). M.J.G. and G.S.-D. would like to thank the support from the Scientific Research Network by the Fonds voor Wetenschappelijk Onderzoek – Vlaanderen (WOG W0014200N).

## Data availability

The data will be shared on reasonable request to the corresponding author.

## References

1. Humbert M, Guignabert C, Bonnet S, Dorfmuller P, Klinger JR, Nicolls MR, Olschewski AJ, Pullamsetti SS, Schermuly RT, Stenmark KR, Rabinovitch M. Pathology and pathobiology of pulmonary hypertension: state of the art and research perspectives. *Eur Respir J* 2019;53: 1801887.
2. Tello K, Naeije R, de Man F, Guazzi M. Pathophysiology of the right ventricle in health and disease: an update. *Cardiovasc Res* 2023;119:1891–1904.
3. Vonk Noordegraaf A, Westerhof BE, Westerhof N. The relationship between the right ventricle and its load in pulmonary hypertension. *J Am Coll Cardiol* 2017;69:236–243.
4. Wessels JN, van Wezenbeek J, de Rover J, Smal R, Llucia-Valdeperas A, Celant LR, Marcus JT, Meijboom LJ, Groeneveld JA, Oosterveer FPT, Winkelman TA, Niessen HWM, Goumans MJ, Bogaard HJ, Noordegraaf AV, Strijkers GJ, Handoko ML, Westerhof BE, de

Man FS. Right atrial adaptation to precapillary pulmonary hypertension: pressure-volume, cardiomyocyte, and histological analysis. *J Am Coll Cardiol* 2023;**82**:704–717.

5. Jiang H, Salmon RM, Upton PD, Wei Z, Lawera A, Davenport AP, Morrell NW, Li W. The prodomain-bound form of bone morphogenetic protein 10 is biologically active on endothelial cells. *J Biol Chem* 2016;**291**:2954–2966.

6. David L, Mallet C, Mazerbourg S, Feige JJ, Baily S. Identification of BMP9 and BMP10 as functional activators of the orphan activin receptor-like kinase 1 (ALK1) in endothelial cells. *Blood* 2007;**109**:1953–1961.

7. Salmon RM, Guo J, Wood JH, Tong Z, Beech JS, Lawera A, Yu M, Grainger DJ, Reckless J, Morrell NW, Li W. Molecular basis of ALK1-mediated signalling by BMP9/BMP10 and their prodomain-bound forms. *Nat Commun* 2020;**11**:1621.

8. Scharpfenecker M, van Dinther M, Liu Z, van Bezooyen RL, Zhao Q, Pukac L, Lowik CW, ten Dijke P. BMP-9 signals via ALK1 and inhibits bFGF-induced endothelial cell proliferation and VEGF-stimulated angiogenesis. *J Cell Sci* 2007;**120**:964–972.

9. Wits M, Becher C, de Man F, Sanchez-Duffhues G, Goumans MJ. Sex-biased TGF $\beta$  signaling in pulmonary arterial hypertension. *Cardiovasc Res* 2023;**119**:2262–2277.

10. International PPH Consortium; Lane KB, Machado RD, Pauciulo MW, Thomson JR, Phillips JA 3rd, Loyd JE, Nichols WC, Trembath RC. Heterozygous germline mutations in BMPR2, encoding a TGF- $\beta$  receptor, cause familial primary pulmonary hypertension. *Nat Genet* 2000;**26**:81–84.

11. Lawera A, Tong Z, Thorikay M, Redgrave RE, Cai J, van Dinther M, Morrell NW, Afink GB, Charnock-Jones DS, Arthur HM, Ten Dijke P, Li W. Role of soluble endoglin in BMP9 signaling. *Proc Natl Acad Sci U S A* 2019;**116**:17800–17808.

12. Goumans MJ, Zwijnen A, Ten Dijke P, Baily S. Bone morphogenetic proteins in vascular homeostasis and disease. *Cold Spring Harb Perspect Biol* 2018;**10**:a031989.

13. Ponikowski P, Voors AA, Anker SD, Bueno H, Cleland JGF, Coats AJS, Falk V, Gonzalez-Juanatey JR, Harjola VP, Jankowska EA, Jessup M, Linde C, Nihoyannopoulos P, Parissis JT, Pieske B, Riley JP, Rosano GMC, Ruilope LM, Ruschitzka F, Rutten FH, van der Meer P; Authors/Task Force Members. 2016 ESC guidelines for the diagnosis and treatment of acute and chronic heart failure: the task force for the diagnosis and treatment of acute and chronic heart failure of the European Society of Cardiology (ESC) developed with the special contribution of the Heart Failure Association (HFA) of the ESC. *Eur Heart J* 2016;**37**:2129–2200.

14. Galie N, Humbert M, Vachiery JL, Gibbs S, Lang I, Torbicki A, Simonneau G, Peacock A, Vonk Noordegraaf A, Beghetti M, Ghofrani A, Gomez Sanchez MA, Hansmann G, Klepetko W, Lancellotti P, Matucci M, McDonagh T, Pierard LA, Trindade PT, Zompatori M, Hoeper M; Authors/Task Force Members. 2015 ESC/ERS guidelines for the diagnosis and treatment of pulmonary hypertension: the joint task force for the diagnosis and treatment of pulmonary hypertension of the European Society of Cardiology (ESC) and the European Respiratory Society (ERS): endorsed by: Association for European Paediatric and Congenital Cardiology (AEPC), International Society for Heart and Lung Transplantation (ISHLT). *Eur Heart J* 2016;**37**:67–119.

15. Livak KJ, Schmittgen TD. Analysis of relative gene expression data using real-time quantitative PCR and the 2( $\Delta\Delta C(T)$ ) method. *Methods* 2001;**25**:402–408.

16. Trip P, Kind T, van de Veerdonk MC, Marcus JT, de Man FS, Westerhof N, Vonk-Noordegraaf A. Accurate assessment of load-independent right ventricular systolic function in patients with pulmonary hypertension. *J Heart Lung Transplant* 2013;**32**:50–55.

17. van de Veerdonk MC, Kind T, Marcus JT, Mauritz GJ, Heymans MW, Bogaard HJ, Boonstra A, Marques KM, Westerhof N, Vonk-Noordegraaf A. Progressive right ventricular dysfunction in patients with pulmonary arterial hypertension responding to therapy. *J Am Coll Cardiol* 2011;**58**:2511–2519.

18. Korchynskyi O, ten Dijke P. Identification and functional characterization of distinct critically important bone morphogenetic protein-specific response elements in the Id1 promoter. *J Biol Chem* 2002;**277**:4883–4891.

19. Morrell NW, Bloch DB, ten Dijke P, Goumans MJ, Hata A, Smith J, Yu PB, Bloch KD. Targeting BMP signalling in cardiovascular disease and anaemia. *Nat Rev Cardiol* 2016;**13**:106–120.

20. Hodgson J, Swietlik EM, Salmon RM, Hadinnapola C, Nikolic I, Wharton J, Guo J, Liley J, Haimel M, Bleda M, Southgate L, Machado RD, Martin JM, Treacy CM, Yates K, Daugherty LC, Shamardina O, Whitehorn D, Holden S, Bogaard HJ, Church C, Coghlan G, Condliffe R, Corris PA, Danesino C, Eryies M, Gall H, Ghio S, Ghofrani HA, Gibbs JSR, Girerd B, Houweling AC, Howard L, Humbert M, Kiely DG, Kovacs G, Lawrie A, MacKenzie Ross RV, Medina S, Montani D, Olschewski A, Olschewski H, Ouwehand WH, Peacock AJ, Pepke-Zaba J, Prokopenko I, Rhodes CJ, Scelsi L, Seeger W, Soubrier F, Suntharalingam J, Toshner MR, Trembath RC, Vonk Noordegraaf A, Wort SJ, Wilkins MR, Yu PB, Li W, Graf S, Upton PD, Morrell NW. Characterization of GDF2 mutations and levels of BMP9 and BMP10 in pulmonary arterial hypertension. *Am J Respir Crit Care Med* 2020;**201**:575–585.

21. Kawel-Boehm N, Hetzel SJ, Ambale-Venkatesh B, Captur G, Francois CJ, Jerosch-Herold M, Salerno M, Teague SD, Valsangiaco-Buechel E, van der Geest RJ, Bluemke DA. Reference ranges ("normal values") for cardiovascular magnetic resonance (CMR) in adults and children: 2020 update. *J Cardiovasc Magn Reson* 2020;**22**:87.

22. Humbert M, Kovacs G, Hoeper MM, Badagliacca R, Berger RMF, Brida M, Carlsen J, Coats AJS, Escribano-Subias P, Ferrari P, Ferreira DS, Ghofrani HA, Giannakoula G, Kiely DG, Mayer E, Meszaros G, Nagavci B, Olsson KM, Pepke-Zaba J, Quint JK, Radegran G, Simonneau G, Sitbon O, Tonia T, Toshner M, Vachiery JL, Vonk Noordegraaf A, Delcroix M, Rosenkranz S; ESC/ERS Scientific Document Group. 2022 ESC/ERS guidelines for the diagnosis and treatment of pulmonary hypertension. *Eur Respir J* 2023;**61**:2200879.

23. Eyries M, Montani D, Nadraud S, Girerd B, Levy M, Bourdin A, Tresorier R, Chaouat A, Cottin V, Sanfiorenzo C, Prevot G, Reynaud-Gaubert M, Dromer C, Houeijeh A, Nguyen K, Coulet F, Bonnet D, Humbert M, Soubrier F. Widening the landscape of heritable pulmonary hypertension mutations in paediatric and adult cases. *Eur Respir J* 2019;**53**:1801371.

24. Sanchez-Duffhues G, Williams E, Goumans MJ, Helden CH, Ten Dijke P. Bone morphogenetic protein receptors: structure, function and targeting by selective small molecule kinase inhibitors. *Bone* 2020;**138**:115472.

25. Chen H, Shi S, Acosta L, Li W, Lu J, Bao S, Chen Z, Yang Z, Schneider MD, Chien KR, Conway SJ, Yoder MC, Haneline LS, Franco D, Shou W. BMP10 is essential for maintaining cardiac growth during murine cardiogenesis. *Development* 2004;**131**:2219–2231.

26. Nakano N, Hori H, Abe M, Shibata H, Arimura T, Sasaoka T, Sawabe M, Chida K, Arai T, Nakahara K, Kubo T, Sugimoto K, Katsuya T, Oghara T, Doi Y, Izumi T, Kimura A. Interaction of BMP10 with Tcap may modulate the course of hypertensive cardiac hypertrophy. *Am J Physiol Heart Circ Physiol* 2007;**293**:H3396–H3403.

27. Neuhaus H, Rosen V, Thies RS. Heart specific expression of mouse BMP-10 a novel member of the TGF- $\beta$  superfamily. *Mech Dev* 1999;**80**:181–184.

28. Mäntymaa P, Vuoleenaho O, Marttila M, Ruskoaho H. Atrial stretch induces rapid increase in brain natriuretic peptide but not in atrial natriuretic peptide gene expression in vitro. *Endocrinology* 1993;**133**:1470–1473.

29. Topper JN, Cai J, Qiu Y, Anderson KR, Xu YY, Deeds JD, Feeley R, Gimeno CJ, Woolf EA, Tayber O, Mays GG, Sampson BA, Schoen FJ, Gimbrone MA Jr, Falb D. Vascular MADs: two novel MAD-related genes selectively inducible by flow in human vascular endothelium. *Proc Natl Acad Sci U S A* 1997;**94**:9314–9319.

30. Llucià-Valdeperas A, Bragos R, Soler-Botija C, Roura S, Galvez-Monton C, Prat-Vidal C, Perea-Gil I, Bayes-Genis A. Unravelling the effects of mechanical physiological conditioning on cardiac adipose tissue-derived progenitor cells in vitro and in silico. *Sci Rep* 2018;**8**:499.

31. Voigt N, Pearman CM, Dobrev D, Dibb KM. Methods for isolating atrial cells from large mammals and humans. *J Mol Cell Cardiol* 2015;**86**:187–198.

32. Owen NE, Nyimana D, Kuc RE, Upton PD, Morrell NW, Alexander GJ, Maguire JJ, Davenport AP. Plasma levels of apelin are reduced in patients with liver fibrosis and cirrhosis but are not correlated with circulating levels of bone morphogenetic protein 9 and 10. *Peptides* 2021;**136**:107440.

33. Hodgson J, Ruiz-Llorente L, McDonald J, Quarrell O, Ugonna K, Bentham J, Mason R, Martin J, Moore D, Bergstrom K, Bayrak-Toydemir P, Woorderchak-Donahue W, Morrell NW, Condliffe R, Bernabeu C, Upton PD. Heterozygous GDF2 nonsense mutations result in a loss of circulating BMP9 and BMP10 and are associated with either PAH or an "HHT-like" syndrome in children. *Mol Genet Genomic Med* 2021;**9**:e1685.

34. Rochon ER, Krowka MJ, Bartolome S, Heresi GA, Bull T, Roberts K, Hemnes A, Forde KA, Krok KL, Patel M, Lin G, McNeil M, Al-Naamani N, Roman BL, Yu PB, Fallon MB, Gladwin MT, Kawut SM. BMP9/10 in pulmonary vascular complications of liver disease. *Am J Respir Crit Care Med* 2020;**201**:1575–1578.

35. Arjaans S, Wagner BD, Mourani PM, Mandell EW, Poindexter BB, Berger RMF, Abman SH. Early angiogenic proteins associated with high risk for bronchopulmonary dysplasia and pulmonary hypertension in preterm infants. *Am J Physiol Lung Cell Mol Physiol* 2020;**318**:L644–L654.

36. Tillett E, Ouarne M, Desroches-Castan A, Mallet C, Subileau M, Didier R, Lioutsko A, Belthier G, Feige JJ, Baily S. A heterodimer formed by bone morphogenetic protein 9 (BMP9) and BMP10 provides most BMP biological activity in plasma. *J Biol Chem* 2018;**293**:10963–10974.

37. Sengle G, Ono RN, Sasaki T, Sakai LY. Prodomains of transforming growth factor beta (TGF $\beta$ ) superfamily members specify different functions: extracellular matrix interactions and growth factor bioavailability. *J Biol Chem* 2011;**286**:5087–5099.

38. Chen H, Brady Ridgway J, Sai T, Lai J, Warming S, Chen H, Roose-Girma M, Zhang G, Shou W, Yan M. Context-dependent signaling defines roles of BMP9 and BMP10 in embryonic and postnatal development. *Proc Natl Acad Sci U S A* 2013;**110**:11887–11892.

39. Sanchez-Duffhues G, Hiepen C, Knaus P, Ten Dijke P. Bone morphogenetic protein signaling in bone homeostasis. *Bone* 2015;**80**:43–59.

40. Reyat JS, Chua W, Cardoso VR, Witten A, Kastner PM, Kabir SN, Sinner MF, Wesseling R, Holmes AP, Pavlovic D, Stoll M, Kaab S, Gkoutos GV, de Groot JR, Kirchhof P, Fabritz L. Reduced left atrial cardiomyocyte PITX2 and elevated circulating BMP10 predict atrial fibrillation after ablation. *JCI Insight* 2020;**5**:e139179.

41. Hijazi Z, Benz AP, Lindback J, Alexander JH, Connolly SJ, Eikelboom JW, Granger CB, Kastner P, Lopes RD, Ziegler A, Oldgren J, Siegbahn A, Wallentin L. Bone morphogenetic protein 10: a novel risk marker of ischaemic stroke in patients with atrial fibrillation. *Eur Heart J* 2023;**44**:208–218.